

# Development of the long-pulse ECRF system for JT-60SA

Takayuki KOBAYASHI<sup>1</sup>, Akihiko ISAYAMA<sup>1</sup>, Damien FASEL<sup>2</sup>, Kenji YOKOKURA<sup>1</sup>, Mitsugu SHIMONO<sup>1</sup>, Koichi HASEGAWA<sup>1</sup>, Masayuki SAWAHATA<sup>1</sup>, Sadaaki SUZUKI<sup>1</sup>, Masayuki TERAKADO<sup>1</sup>, Shinichi HIRANAI, Koichi IGARASHI<sup>1</sup>, Fumiaki SATO<sup>1</sup>, Kenji WADA<sup>1</sup>, Minoru SHIBAYAMA<sup>1</sup>, Jun HINATA<sup>1</sup>, and Shinichi MORIYAMA<sup>1</sup>

<sup>1</sup>Japan Atomic Energy Agency, Naka, Ibaraki, Japan

<sup>2</sup>Centre de Recherches en Physique des Plasmas, Lausanne, Switzerland

(Received: 12 November 2009 / Accepted: 22 April 2010)

Improvements of the Electron Cyclotron Range of Frequency (ECRF) system in JT-60U and design works are underway towards steady-state operation in JT-60SA. Since the ECRF system in JT-60U was designed as a 5 s system, improvements in almost all the system are required to achieve the target pulse length of 100 s with a gyrotron output power of 1 MW for JT-60SA. The issues and present status of the design and development are summarized from a view point of requirements for obtaining long pulse ECRF system.

Keywords: long-pulse ECRF system, JT-60SA

## 1. Introduction

Design and development of an Electron Cyclotron Range of Frequency (ECRF) system for JT-60SA is underway. A phased construction concept consisting of initial, integrated and extended research phases is applied for JT-60SA [1, 2]. In the initial research phase, the ECRF system will provide an injection power of 1.5 MW for 100 s using two gyrotrons and additional 1.5 MW for 5 s using the other two gyrotrons. In the integrated research phase, an injection power of 7 MW for 100 s will be provided using nine gyrotrons. Nominal output power of each gyrotron is 1 MW. Each gyrotron has an evacuated waveguide transmission line. Four launchers will be installed on the upper oblique ports of the JT-60SA tokamak for the nine transmission lines. The millimeter-wave frequency is 110 GHz which is the same as that used in JT-60U. Since the ECRF system developed for the JT-60U [3] was designed for obtaining pulse length of 5 s at a gyrotron output power of 1 MW, improvements are required in many components of the system for achieving pulse length of 100 s. In the initial research phase, two units of power supplies are fabricated and installed by EU. The two 100 s gyrotrons (110 GHz) are procured by JA. Two units of the power supplies and gyrotrons used in JT-60U will be used for 5 s units as they are. Since the frequency of the output millimeter-wave in JT-60SA is the same as that in JT-60U, four superconducting magnets ( $B < 4.5$  T) can be reused. Four transmission lines and two launchers are installed by JA.

The requirements of the improvements on the JT-60 ECRF system had been discussed between JAEA and EU in recent two or three years. This paper aims at to clarify such requirements on each ECRF system component (gyrotron, power supply, transmission line, launcher and

others) for obtaining the long pulse of 100 s in JT-60SA, and to show the progress of the design and developments of the system mainly about the gyrotron, transmission line and launchers those need some R&D, and plans for near future toward JT-60SA using the JT-60 ECRF system. We do not discuss the system for the integrated research phase in this paper.

## 2. Power Supply

DC Generator primary AC voltage	18 kV
Secondary DC voltage	-65 kV
DC current	65 A
Voltage ripple	< 1%
Duty cycle	1/18
Fast DC switch shutoff	< 10 micro s
Modulator frequency	> 5 kHz
Acceleration power supplies	
DC voltage	50 or 90 kV
DC current	0.3A CW
Voltage ripple	< 0.5%

Table 1 Design specification of the ECRF power supply in the initial research phase.

The power supplies used on the JT-60U ECRF system limited the pulse duration to 30 s even with the reduced output power of 0.4 MW [4]. Newly developed power supplies will be fabricated and installed by EU enabling pulse length of 100 s at 1 MW in the initial research phase. Since the JT-60 gyrotron equips a triode type magnetron ignition gun (MIG) with a collector potential depression technology, the power supply will consist of a main high voltage power supply (MHVPS), body power supply (BPS) and anode power supply (APS) or anode voltage

divider (AVD). The design specification of the power supplies is shown in Table 1 [5]. The choice of the gyrotron supply topology is one of the major issues, since the BPS and the APS (AVD) can be either referred to the cathode, or independently referred to the collector (ground) for the BPS and to the cathode for the APS (AVD). A selection between these two topologies will occur in a near future. However, a 100 s operation at a nominal operation parameter (the voltage and the current of each power supply) for 1 MW will not have a significant technical difficulty by each topology. A detailed discussion between EU home team and Japanese home team will be continued in order to define the detailed specifications.

### 3. Gyrotron

A 110 GHz gyrotron used in JT-60U was originally designed for obtaining 1 MW output power with a pulse length of up to 5 s. After achieving the target output power of 1 MW for 5 s [6], improvements of the gyrotron and peripheral equipments for obtaining longer pulse length and higher power had been continued. For example, a large sized DC-break made of an alumina ceramic between body electrode and collector electrode was replaced with that made of a  $\text{Si}_3\text{N}_4$  ceramic due to its property of high thermal strength and low rf absorption rate. Flow rates of cooling waters at some internal components were increased. The longest pulse length of 30 s was successfully achieved in an experimental campaign of JT-60U in 2007 with a reduced output power of 0.4 MW. A reduction of diffracted rf power loss in the gyrotron and an increase in the oscillation efficiency are mainly required for achieving a pulse length of 100 s at 1 MW for the gyrotron.

For reducing the diffracted power in the gyrotron, an improved 110 GHz gyrotron was fabricated in 2008. The gyrotron equips a newly designed built-in mode convertor in order to reduce the stray radiation power in the gyrotron. The previous mode convertor consisted of a single helix type launcher and quasi-optical mirrors including a pair of phase correction mirrors. The new launcher was designed by means of the Launcher Optimization Tool (LOT) [7, 8]. The launcher has a complicated wall shape optimized by the LOT. Moreover, the new mode convertor does not have phase correction mirrors in order to reduce risk of deformation of phase pattern at the window due to misalignment of those mirrors in fabrication process. The technique used for designing the mode convertor was the same as that used in designing a 170 GHz gyrotron for ITER in JAEA, which achieved an oscillation of 1 MW for 800 s [9]. Gyrotrons designed with the same technology have been fabricated for the large helical device and the GAMMA 10 tandem mirror at frequencies of 77 GHz and 28 GHz, respectively [10-12]. As studied in Ref. 10, the lower frequency can cause problems due to large amount of diffraction loss even with the same technology. If such

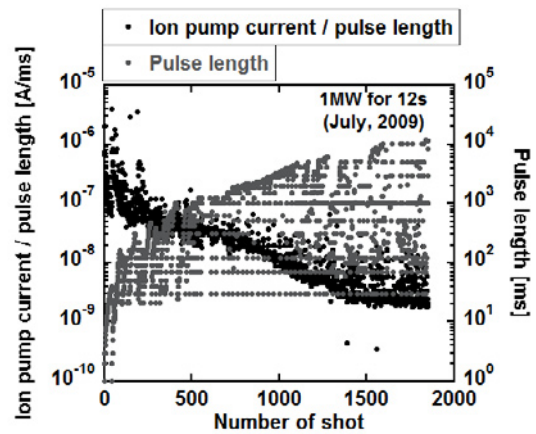


Figure 1 Progress of the collector conditioning of the improved gyrotron.

problems come up for the 110 GHz gyrotron in long pulse operation, additional counter measures are required for JT-60SA. Therefore, an experimental verification of the effectiveness of the improvement was essential for the 110 GHz gyrotron. For testing the newly fabricated gyrotron at long pulse, a MHVPS previously used for the Lower Hybrid (LH)-A system in JT-60U was connected to the ECRF system in 2009. Since the current capacity of the LH-A system (60 kV/130 A) is higher than that of the previous ECRF system (60 kV/65 A) by a factor of two, the gyrotron can be tested at long pulse of at least 30 s with an operation current of less than 65 A. The conditioning operation of the gyrotron has already been started. Figure 1 shows a progress of conditioning of the gyrotron. As ion pump current of the gyrotron, which was a measure of the gas pressure in the gyrotron, decreased, the pulse length increased without a hitch. The pulse length at an output power of 1 MW has been reached to 12 s within five months of conditioning operation (July, 2009). The pulse length was significantly longer than the pulse length achieved in ten years operations in JT-60U by the previous gyrotrons (5 s at 1 MW), and no significant increase of the gas pressure in the gyrotron was observed. The extension of the pulse length is expected in near future toward 100 s after confirming the feasibility of the transmission line that was modified as described in the following section.

Although the highest oscillation efficiency achieved by the JT-60 gyrotron was close to 50% at short pulse [6], the efficiencies at the operations in JT-60U experiments were 40% or lower. This fact was mainly caused by a large amount of the ripple voltage of the MHVPS used in JT-60U which was originally designed for the Lower Hybrid (LH)-system, and therefore, reduction of the efficiency was needed for obtaining stable oscillation using such a power supply. It is, however, expected that the MHVPS newly designed by EU will provide lower ripple voltage than that of the previous one and it may result in obtaining high efficiency of around 50% in an ideal situation. The gyrotron may be sometimes operated with

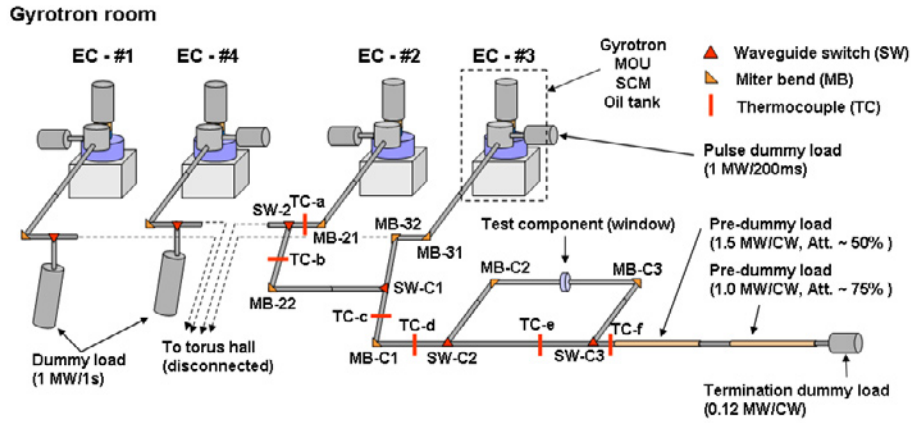


Figure 2. Schematic view of the transmission line of the ECRF system in the JT-60 gyrotron room in 2009. A waveguide type dummy load system is shared by EC-#2 and EC-#3 units by the use of a waveguide switch (SW-C1).

reduced oscillation efficiency when the ideal situation is not obtained due to some experimental reasons (for example, gyrotron arcing, electrical noises due to other devices, and insufficient time for optimization). Therefore the gyrotron may be operated with an efficiency range of 30% (worst case) to 50% (ideal case). Such an improvement of the maximum oscillation efficiency in an ideal condition is favorable from the viewpoint of the failure cycle of the collector. The improvement of the mode convertor described above may also give higher efficiency, and further improvements of gyrotron itself may be carried out.

#### 4. Transmission line

In JT-60SA, waveguide transmission lines connect the gyrotrons in the gyrotron room and the launchers at the tokamak. Since we have many 31.75 mm/60.3 mm waveguide components (waveguide, miter-bend, window, DC-break, gate-valve, dummy load, and so on) used in JT-60U, the candidates of the waveguide diameter for JT-60SA are also 31.75 mm and/or 60.3 mm for reducing construction cost. The theoretical loss on the waveguide for HE<sub>11</sub> mode of 31.75 mm and 60.3 mm are 6.7%/100 m and 0.71%/100 m, respectively [13, 14]. However, the practical transmission loss on the waveguides strongly depends on a mode conversion at miter-bends or that caused by a misalignment of the transmission line. The number of the miter-bends is expected to be seven to nine per line in JT-60SA. The theoretical mode conversion loss for one miter-bend of 31.75 mm and 60.3 mm are 1.4% and 0.5%, respectively, and one-half of them are expected to be higher order mode that heats the waveguides near the miter-bend locally. The mode conversion loss due to misalignment of the waveguide of the large diameter component is relatively large compared with that of the small diameter component while the excited mode is expected to be lower order mode and it can propagate long distance with low attenuation. Therefore, the large diameter of 60.3 mm is desired for eliminating local heating of the waveguide components and for reducing total loss of the HE<sub>11</sub> mode.

Since the diameter of 60.3 mm is very close to that of waveguides in ITER (63.5 mm) and the similar design of ITER transmission line components is applicable also for 60.3 mm components, a design work of such a large sized diameter components may not be a major issue.

On the other hand, the use of 31.75 mm waveguides can reduce construction cost of the ECRF system in JT-60SA especially in the gyrotron room where the maintenance is relatively easy compared with maintenance in the torus hall. In this case, the waveguides close to miter-bends must be cooled externally. The theoretical loss of the HE<sub>11</sub> mode for 31.75 mm waveguide is 0.69 kW for 1 m at the transmitted power of 1 MW. The heat capacity per unit length of the 31.75 mm waveguide made of aluminum is 1.7 kJ m<sup>-1</sup> K<sup>-1</sup>, thus, the expected temperature rise for 100 s is about 40 °C assuming adiabatic condition; it is acceptable level. Consequently the external cooling for the waveguides away from the miter-bends may not be required if the heat deposition due to higher order mode is well localized around the miter-bends. It is, however, recognized that the practical loss on the waveguide sometimes differs from the theoretical one. A quantitative evaluation of the distribution of the temperature rise on the waveguide transmission line has not been done sufficiently. Therefore an experimental evaluation of the deposition length of the higher order mode excited at the miter-bend and a measurement of the practical loss on the waveguide are essential for confirming the availability of the 31.75 mm waveguides and for designing the cooling system.

Since the JT-60U experiments was finished in 2008 and disassemble will be started soon (in 2010), the transmission line in the torus hall was separated from the transmission line in the gyrotron room. This modification enables us to test transmission line components at high power using a dummy load system (1 MW for continuous wave (CW) operation) in the gyrotron room independently of disassembling of the JT-60U tokamak. Figure 2 shows a schematic view of the transmission line in the gyrotron room at present. A waveguide type dummy load system, which consists of a pre-dummy-load, pumping waveguide,

dummy-load and termination-load is shared by the EC-#2 and EC-#3 using a waveguide switch (SW-C1). The flow rate of the cooling water of the termination load, which was originally used as a short pulse load (1 MW/0.2 s at 10 L/min) was increased to  $\sim 40$  L/min which gives a capability of 0.12 MW for CW operation. In addition to the main transmission line (direct connection from the miter bend (MB-C1) to the dummy load system, a roundabout route is installed between the MB-C1 to the pre-dummy load using two waveguide switches (SW-C2 and SW-C3) and it will be used for testing high power capability of some components such as a window and polarizer. At present, 31.75 mm diameter components are installed and tested. They will be replaced with 60.3 mm diameter components after sufficient measurements are carried out with the present transmission line.

Since the waveguide is made of aluminum and its emissivity is too low, the temperature was measured by means of an Infra-Red (IR) camera with a tape of which emissivity was known ( $\sim 0.95$ ). Thermocouples (TCs in Fig. 2) were also installed at the center of the outer surface of the waveguides and the backward surface of the miter bend mirrors.

An experiment was performed with a gyrotron output power of 0.45 MW for 10 s using EC-#2 unit. The temperature rise of the miter-bend mirror, which was actively cooled by water, was acceptable level for 100 s operation at 1 MW as discussed in the previous work [4]. The temperature of the waveguide, which was not cooled actively, was increased almost linearly and kept the peak temperature for several tens of seconds or longer as shown in Fig. 3. Figure 4 shows the distribution of the temperature rise of the waveguides (not including Matching-Optics-Unit (MOU), miter-bends, switches and waveguide couplings) measured by the IR-camera. The highest temperature rise of about 15 °C was observed just after the SW-2, and the temperature rise of other points close to the miter-bends and switches were also relatively high  $\sim 10$  °C as expected. Although the temperature rise estimated by the theoretical loss of the HE<sub>11</sub> mode was 1.8 °C for transmitted energy of 4.5 MJ with adiabatic condition, the observed temperature rise exceeded 1.8 °C elsewhere; it was typically 5 °C which corresponds to 100 °C for the case of 100 s operation at 1 MW. It seems like too high for repetitive operations. The longest length of the straight lines was about 9 m (between the MB-C1 and dummy load) in this experiment (neglecting the SW-C2 and SW-C3 those were used as short gaps). This result suggested two possibilities. One is that the length of over 5 m was required for absorbing the higher order mode excited at the MB-C1. The other is that there was a large amount of lower order mode. It was difficult to identify the origin of such a mode conversion loss. Therefore, we will try to observe the temperature rise with longer transmission line and also try to observe temperature rise by changing

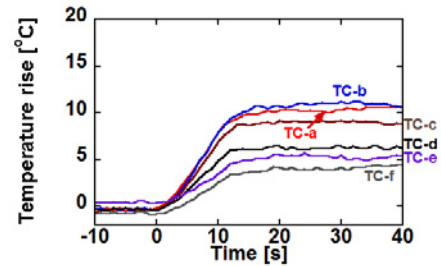


Figure 3 Temperature rises of the waveguides measured by thermocouples installed at the center of the waveguides as shown in Fig. 5. The gyrotron output power and pulse length are about 450 kW and 10 s, respectively.

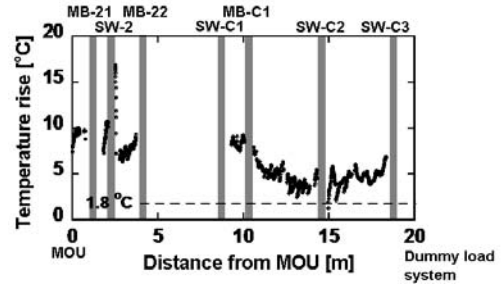


Figure 4 Distribution of temperature rise of the waveguides measured by an IR-camera. The theoretical temperature rise for pure HE<sub>11</sub> mode is 1.8 °C for the 31.75 mm waveguides made of aluminum.

the coupling of the rf beam into waveguide at the MOU actively in near future in order to clarify the localization of the heat deposition near the MOU. The total absorbed power on the waveguides (except miter-bends, coupling components, and MOU) was about 25 kW which was estimated by connecting the temperature of the waveguides smoothly where measured temperature was not obtained. The adiabatic condition was also assumed. This power corresponds to about 6% of the transmitted power. In practice, the temperature should be affected by the cooling at the miter-bend, radiation cooling, and the heat capacities of the miter-bend housings and waveguide couplers, and the adiabatic condition was not satisfied. Thus, the above estimation gives lower limitation.

Nevertheless, it was clarified that the waveguide at least 5 m from the miter-bend was needed to be cooled externally for long pulse transmission at 1 MW in this condition. Since this condition is close to that expected for the transmission line in the gyrotron room in JT-60SA, many part of the waveguides in the gyrotron room require the external cooling for the use of 31.75 mm waveguides. The requirement of flow rate of the cooling water for the waveguide with a transmission loss of 6% is about 43 L/min even for a continuous wave operation at 1 MW assuming the water temperature rise of 20 °C. Moreover, the JT-60SA is pulsed operation of 100 s with duty cycle of 1/18. Therefore, the flow rate of the cooling water is not major issue in the gyrotron room where the water flow lines for an ion cyclotron range of frequency heating system (8400 L/min) and a lower hybrid current drive

system (2870 L/min) in JT-60U can be used for the ECRF system in JT-60SA. Further experiments for confirming the localization of the temperature rise near the MOU and the temperature distribution on the longer transmission line are planned in near future for discussing the availability of the 31.75 mm waveguides in the torus hall.

### 5. Launcher/Antenna

Since maintenance of the components in the vacuum vessel is difficult due to higher neutron fluence in JT-60SA than that in JT-60U, highly reliable cooling and driving mechanism are required for the antenna which is used for altering the ECRF beam direction in both poloidal and toroidal directions. A newly proposed Linear Motion-antenna (LM-antenna) [15] using a linearly-driven small mirror (M1) and a large fixed-curved mirror (M2) has an advantage of reducing risks of water leakage and fault of the driving mechanism in the vacuum by eliminating flexible tubes for coolant supply and link mechanisms for rotating mirror to alter the poloidal beam direction in the vacuum vessel.

Optical characteristics of this antenna have to be clarified because the curvature of M2 is not designed for obtaining focused beam in a plasma but designed for altering beam angle in wide poloidal range. In order to clarify this issue, a preliminary designed was carried out. The calculated result showed that a wide range of poloidal

injection angle is obtained with a reasonable beam width [16], e.g. the beam radius of less than 10 cm is required for neoclassical tearing mode stabilization at the poloidal injection angle of around 40°, which is almost comparable to the beam width in JT-60U. Moreover, mock-up mirrors made of aluminum were fabricated for evaluating the optical characteristics by low-power measurements. The curvature of M2 is 700 mm and M1 is flat mirror in this mock-up antenna. The width and height of M1 and M2 are 120 mm x 150 mm and 400 mm x 275 mm, respectively. Figure 5 shows an example of a comparison between measured millimeter-wave power distribution and calculated one at the poloidal angle,  $\alpha$ , and the distance from the port edge of  $\alpha = 0^\circ$  and  $z = 500$  mm, respectively. It was clarified that the measured power distribution was well consistent with the calculated one, except the interference pattern on the measurement due to reflection from the measurement system. Therefore, it was confirmed that the design based on the numerical calculation [13] can be adopted for the optimization of the antenna design for JT-60SA.

The next important step on the launcher is mechanical design of the launcher and its testing. In order to move the M1 by around 400 mm in front of the waveguide end, a long-stroke bellows, bearing and support are required. Moreover, additional movable axis is required for altering the beam angle in toroidal direction. At present, an idea has been proposed. In addition to the long-stroke shaft (main-shaft for linear motion), another shaft (sub-shaft for rotation) is connected to the main-shaft as shown in Figure 6 with T-shape. By turning the sub-shaft on the side vertical to the main shaft, the main-shaft rotates around its linear motion axis and resulting in the rotation of M1. The M1 rotates around the axis of the main-shaft, not around waveguide axis in this concept. The cooling water for M1 inputs from the top of the sub-shaft and through the main-shaft, the waver cools the M1 and backs through the main and sub-shafts again. The mechanical design has been started in the middle of 2009 and the cooling capability of those mirrors will be evaluated by the use of commercially available Finite Element Method (FEM) code. The support structure will be designed after the basic design of the launcher is carried out.

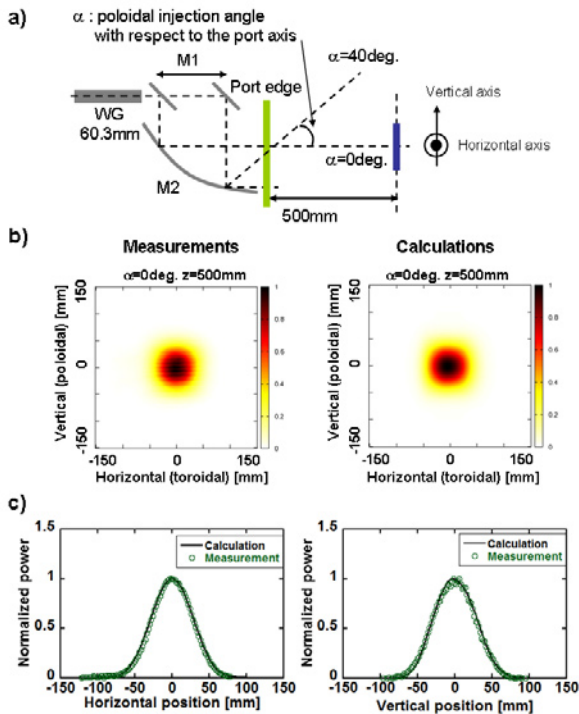


Figure 5. Comparison between low power measurement and calculation for the mock-up antenna. (a) shows an experimental setup. (b) shows measured (left) and (calculated) power distributions at 500 mm from the port edge and  $\alpha = 0^\circ$ , and (c) shows comparisons at the horizontal (left) and vertical (right) cross sections of them at the center of each profile.

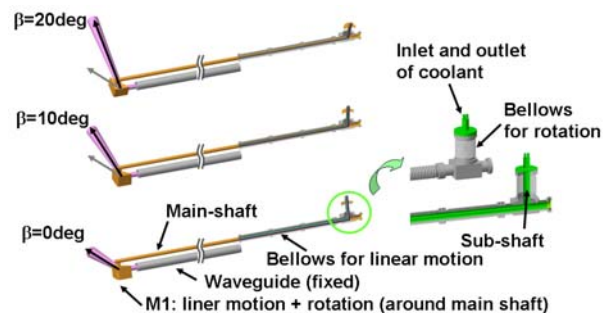


Figure 6. Conceptual drawing of a toroidal rotation mechanism of the movable mirror. The rotation of M1 is realized by turning the sub-shaft vertically to the main shaft.

## 6. Control and Data Acquisition

Since an ECRF system is an essential tool rather than a system for proof of principle, a control system is more important in JT-60SA than that in JT-60U. From the view point of long-pulse gyrotron operation, the gyrotron should be always operated with a high total efficiency of around 50%. Even for a fixed power operation, pre-programmed and/or feedback controls of heater current and anode voltage will be required because the beam current decreases due to cathode cooling by electron emission resulting in the changing of the oscillation condition of the gyrotron during a shot. These control techniques have been successfully developed using the JT-60U ECRF system [4] and the control units will be upgraded for JT-60SA.

Moreover, it is expected that the real-time (feedback and/or pre-programmed) control of the cavity magnetic field, cathode, anode and acceleration voltages can be used for the slow output power modulation during a shot if such an operation is required for feedback control of electron heating power and driven current. Response times of voltages, magnetic field and cathode heater are roughly orders of 1 ms, 1s, and 10 s, respectively, except the case of fast power modulation for the neoclassical tearing mode stabilization.

The data acquisition system will be newly designed to obtain operation data at long pulse of 100 s or longer. Since, however, the longest acquisition time of the ECRF system in JT-60U was 65 s, the expansion of the pulse length to 100 s does not cause significant difficulty.

Techniques and devices for control and data acquisition systems will be improved every year. Consequently the detailed design and fabrication of the system will be done at two or three years before it is used in JT-60SA.

## 7. Summary

The requirements of improvements on the ECRF system and the present status of the design and development for achieving a pulse length of 100 s at 1 MW per line in JT-60SA were shown. For the power supply which is fabricated and installed by EU, selection of a topology is a major topic but the achievement of 100 s at a nominal operation parameter will be possible by each topology. For the gyrotron, reduction of the diffraction loss in the gyrotron and improving the oscillation efficiency are required. In order to reduce diffraction loss in the gyrotron, improved gyrotron equipping a newly designed mode convertor was fabricated and the conditioning operation has been started. The pulse length reached 12 s at 1 MW (July, 2009) without significant trouble. The higher oscillation efficiency is expected by means of newly designed power supply for an ideal case which is favorable from the view point of the failure cycle of the collector. For the transmission line, the use of a 60.3 mm diameter

waveguide will give a capability of a long pulse operation at 1 MW. On the other hand, the use of a 31.75 mm diameter waveguide at a part of the transmission line has also been considered for reducing construction cost. A high power experiment for evaluating temperature rise of waveguide components was carried out and it was suggested that the waveguide at least 5 m from the miter-bends needed to be cooled externally. For the antenna/launcher, a confirming an optical characteristic of a newly proposed antenna concept of the LM-antenna and a designing of a mechanical structure were important issues. A low power test using mock-up antenna mirrors was carried out for confirming the reliability of the numerical design and the measured profile was agreed with the calculated profile. The next important step in near future is a designing the mechanical structure of the launcher including its support structure, and the toroidal rotation mechanism was proposed. For the control and data acquisition system, a concept of the pre-programmed control system developed in JT-60U and additional feedback/pre-programmed system will be needed in JT-60SA for achieving long pulse with high efficiency. The control system and data acquisition system will be designed in detail and fabricated at two or three years before operation of the system in JT-60SA.

## Acknowledgements

The authors would like to thank Drs. K. Sakamoto, A. Kasugai, K. Takahashi, K. Kajiwara and Y. Oda in JAEA for useful discussion on the ECRF system in JT-60.

## References

- [1] T. Fujita, Proc. of 36th EPS conference on Plasma Physics, P4.172 (2009).
- [2] S. Moriyama *et al.*, Proc. of 34th IRMMW-THz, 0442 (2009).
- [3] Y. Ikeda *et al.*, Fusion Sci. Technol. **42**, 436 (2002).
- [4] S. Moriyama *et al.*, Nucl. Fusion **49**, 085001 (2009).
- [5] B. Spears, Plant Integration Document v.2.2 (2009).
- [6] K. Sakamoto *et al.*, Nucl. Fusion **43**, 729 (2003).
- [7] R. Minami *et al.*, J. Infrared. Millim. Waves **27**, 13 (2006).
- [8] J. Neilson and R. Bunger, Proc. of 28th IRMMW, Th5-6, 377 (2003).
- [9] K. Sakamoto *et al.*, Nature Phys. **3**, 411 (2007).
- [10] T. Imai *et al.*, Proc of 22nd IAEA FEC, IAEA-CN-165 /FT/P2-25 (2008).
- [11] T. Shimozuma *et al.*, Proc. of the 18th Topical Conference on Radio frequency power in plasmas, 479 (2009).
- [12] H. Takahashi *et al.*, Fusion Sci. Technol. **57**, 19 (2009).
- [13] J. L. DOANE and R. A. OLSTAD, Fusion Sci. Technol. **53**, 39 (2008).
- [14] J. L. DOANE, Fusion Sci. Technol. **53**, 159 (2008).
- [15] S. Moriyama *et al.*, Fusion Eng. Des. **82**, 785 (2007).
- [16] T. Kobayashi *et al.*, Fusion Eng. Des. **84**, 1063 (2009).